Bull. Spec. Astrophys. Obs., 2003, 55, 5–17

Iron abundance in the atmospheres of components of the binary system 41 Draconis

Yu.Yu. Balega[a], V.V. Leushin[a], G. Weigelt[b]

[a] Special Astrophysical Observatory of the Russian AS, Nizhnij Arkhyz 369167, Russia
[b] Max-Plank Institute of Radioastronomy, Bonn, Germany

Received January 16, 2003; accepted February 5, 2003.

Abstract.
Iron abundances, FeI and FeII lines equivalent widths, and microturbulence velocities were found for the components of a highly eccentric spectroscopic and interferometric binary system 41 Dra from high resolution spectra obtained close to the periastron. Weighted mean values of iron abundances in the atmospheres are lgN(Fe) = 7.66 ± 0.03 and $lgN(Fe) = 7.72 \pm 0.03$ for the component *a* and *b*, correspondingly. These values are approximately 0.2 dex higher than the solar iron abundance. The flux ratio, measured from the depths of FeI and FeII lines, $E^b/E^a = 0.7$, is in agreement with the magnitude difference $0^m.41$ found recently by speckle interferometry. It is supposed that the weaker companion of the binary has slightly higher effective temperature.

Key words: stars: binaries – stars: atmospheres — stars: abundances

1. Introduction

Stellar chemical composition provides information about the origin and evolution of a star. However, to estimate the chemical composition of a stellar atmosphere one needs first to define fundamental properties of the star. Precise parallax, if known, allows in that case an independent determination of the stellar luminosity and effective temperature. For a binary star, the main parameters, masses and radii, can be directly obtained from the analysis of the orbital motion.

All these possibilities are presented for the unique binary star 41 Dra, which is at the same time a member of the quadruple system ADS 11061. The binary shows the highest eccentricity among spectroscopic binaries 0.9754 and is of great interest for the theories of origin and evolution of hierarchical multiple systems, tidal interactions and dissipative orbit circularization (Balega et al. 1997).

The orbital period of 41 Dra is 3.41 year with a semimajor axis 3 AU and a periastron separation between the components of about 10 stellar radii. The binary shows the F7 spectral type with $B-V = 0.51$, while their masses lie in the range $1.2 - 1.3\,M_\odot$. The quadruple system is at the distance 45 pc from the Sun.

Most of the orbital period, the components of 41 Dra move with small velocity difference, and their spectral lines are not blended. Only close to the periastron passage, when the velocities are fast increasing, one can observe complete line separation in the spectrum. This interval is rather short, close to ±15 days from the periastron, or 0.03 of the orbital period. Therefore, most of the period, we can study the star in its stationary state. Comparison of the spectra in the stationary state and close to periastron allows discovering possible interaction effects between the components. In the present work we have made a detailed analysis of the iron lines in the spectra of both components of 41 Dra taken at the system periastron in June 2001.

2. Parameters of the components

In the previous studies of 41 Dra based on speckle interferometric and spectroscopic observations, we have separated the continuum spectra of the components and defined their atmospheric parameters (Balega et al. 2001):

$$M^a = 1.48 M_\odot, T^a_{eff} = 6575\,\mathrm{K},$$
$$\lg g^a = 4.08, R^a = 1.820\,R_\odot;$$
$$M^b = 1.40 M_\odot, T^b_{eff} = 6600\,\mathrm{K},$$
$$\lg g^b = 4.26, R^b = 1.460\,R_\odot.$$

These parameters give the correct description of most available observational data. The effective temperature error does not exceed ±200 K, while for the surface gravity the uncertainty is $\Delta \lg g = \pm 0.1$. Probably the parameters difference is real and reflects the

difference of the physical properties and evolution status of the components.

3. Observations

The analysis of the atmospheres of the 41 Dra components was performed using the high resolution spectra obtained at the 6 m (BTA) telescope, 2 m Zeiss telescope at Peak Terskol, and 1 m telescope of the observatory (Musaev 1993; Panchuk et al. 1998). The list of the spectra under study is given in Table 1.

Some of the analyzed spectra are shown in Fig. 1. Here are presented both the unnormalized spectra (b, e) and the spectra normalized to the continuum (a, c, d). The spectra were obtained during the system approach to the periastron showing the increase of the relative velocity of the components. In 2000, spectral lines showed only small asymmetry in their blue wings, while starting from February 2001 the lines separation became absolutely clear.

Speckle interferometric measurements showed that the magnitude difference between the components is

$$\Delta m = 0.33 + 0.9 \cdot 10^{-5}[\text{Å}^{-1}] \cdot \lambda[\text{Å}]$$

with the mean value in the used wavelength interval $\Delta m = 0.41$ ($E^b/E^a = 0.68$), thus giving the evidence that the weaker b-component has a higher effective temperature. The analysis of spectral lines also gives an opportunity to estimate the brightness ratio of the components. In the case when the effective temperatures are similar, the ratio of the line central depths is connected to the brightness ratio by the equation:

$$E_\lambda{}^b/E_\lambda{}^a = (R_c{}^a + R_c{}^b)/R_c{}^a - 1.$$

Here $R_c{}^a$ and $R_c{}^b$ are the central depths of the resolved lines.

In Fig. 2 the ratio $E_\lambda{}^b/E_\lambda{}^a$ is plotted vs. wavelength.

The obtained relationship

$$E_\lambda{}^b/E_\lambda{}^a = 0.73 - 0.54 \cdot 10^{-5}[\text{Å}^{-1}] \cdot \lambda[\text{Å}]$$

confirms both the mean brightness ratio and the possible rise of Δm with wavelength, thus supporting the idea of higher effective temperature for the weaker component b.

4. Equivalent widths of FeI lines

FeI lines are the most numerous in the spectra of both components of 41 Dra giving possibilities for the detailed study of physical conditions in their atmospheres. For the analysis we used the spectra obtained in the period 12.01.2001–12.04.2001 when spectral

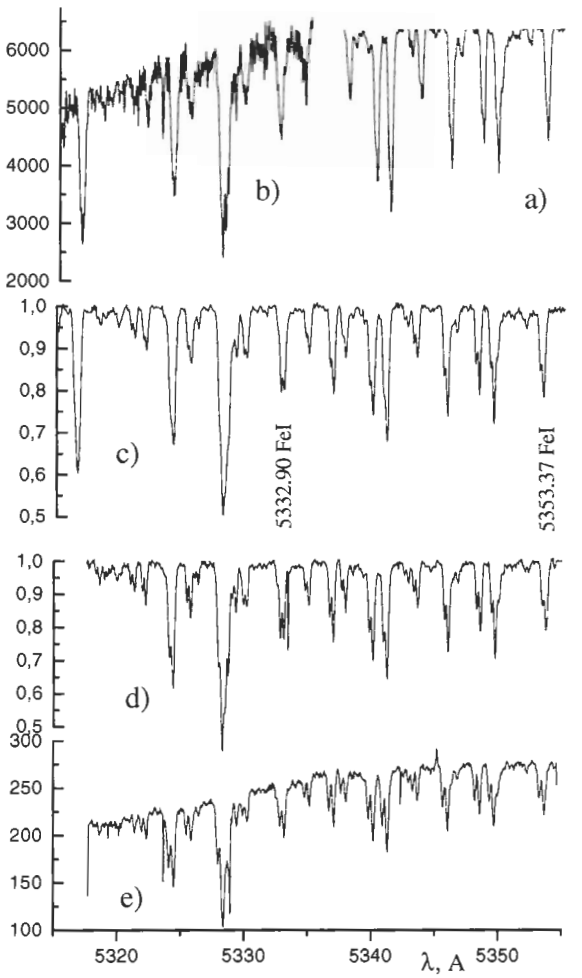

Figure 1: *A comparison of 41 Dra spectra for different dates: a) spectrum t053123 on 13.11.2000, b) Z3818 on 14.11.2000, c) L01 on 11.12.2000, d) L09 from 07.02.2001, e) L02 on 16.04.2001.*

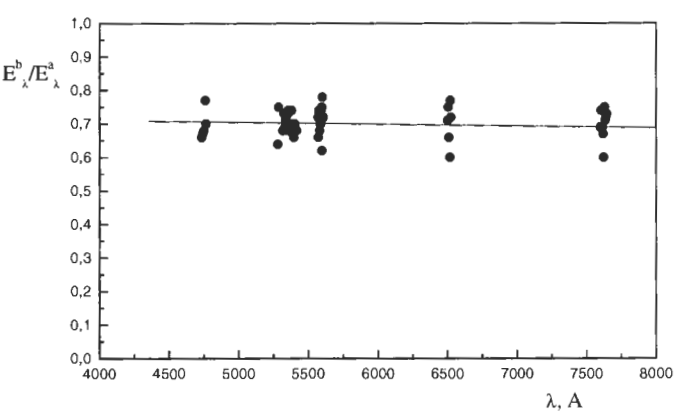

Figure 2: *Component brightness ratio as a function of the wavelength. E_λ^b/E_λ^a is derived from measurements of R_c^a and R_c^b.*

Table 1: *List of 41 Dra spectra*

Date	Telescope	Spectrogr.	Number	Sp.region	Resolut.	S/N	V_r^a km/s	V_r^b km/s
10.11.2000	BTA	MSS	o01	4263-4425	15000	200	11.8	0.1
	BTA	MSS	o04	4748-4909	15000	400		
	BTA	MSS	o05	4454-4616	15000	400		
	BTA	MSS	o08	4454-4616	15000	200		
	BTA	MSS	c3992	3990-4155	15000	200		
	BTA	MSS	c3992	3990-4155	15000	200		
	BTA	MSS	c3992	3990-4155	15000	200		
13.11.2000	BTA	MSS	o01	4450-4616	15000	250	11.9	0.1
	BTA	MSS	o04	4550-4860	15000	350		
	BTA	MSS	o05	4450-4616	15000	250		
	Zeiss(2 m)	CEGS	t053123	3700-8000	100000	100		
	Zeiss(2 m)	CEGS	t05412	3700-8000	100000	100		
14.11.2000	Zeiss(1 m)	CEGS	Z3818	4120-9159	100000	200	11.9	0.0
	Zeiss(1 m)	CEGS	Z3819	4120-9159	100000	200		
11.12.2000	BTA	NES	L01	4862-5720	40000	250	12.5	-0.5
12.12.2000	BTA	MSS	O11	4451-4614	15000	250	12.5	-0.6
12.01.2001	BTA	MSS	o0203	3993-4155	15000	150	13.2	-1.3
	BTA	MSS	o0405	4262-4425	15000	150		
	BTA	MSS	o0809	4774-4938	15000	400		
07.02.2001	BTA	NES	L09	4686-5541	40000	250	14.0	-2.1
06.04.2001	BTA	NES	L02	4733-5606	40000	250	16.6	-4.9
12.04.2001	BTA	NES	o03	4450-4615	40000	250	16.9	-5.3

lines were well separated. Similar effective temperatures of the components lead to similar absorption line intensities in the spectra. For both components this circumstance strongly simplifies the procedure of lines separation and their equivalent widths determination. If the brightness ratio between the components is

$$l = {E_\lambda}^b / {E_\lambda}^a,$$

then the equivalent line widths for the a and b component are

$$W_\lambda^a = {W_{\lambda,obs}}^a (1+l),\ {W_\lambda}^b = {W_{\lambda,obs}}^b (1+l)/l.$$

With a mean value of $l = 0.68$ this gives

$$W_\lambda^a = 1.68 W_{\lambda,obs}^a$$

and

$$W_\lambda^b = 2.50 W_{\lambda,obs}^b.$$

We use these W_λ and R_c values below.

In Tables 2 and 3 the lists of FeI lines in the spectral region $\lambda\lambda 5260 - 5605$ ÅÅ are presented for the dates 07.02.2001 and 06.04.2001 together with their parameters and equivalent widths. The processing of the spectra was performed using the software DECH20 (Galazutdinov 1992). The equivalent widths for the two above mentioned dates are compared in Figs. 3 and 4. Fig. 5 gives the comparison of the central line depths for the two components. There is no significant difference in the line depths, however the regression

$$R_a = 0.833 \cdot R_b + 0.048$$

shows that the depth of strong lines in b component is slightly larger than that in a component.

This effect can be caused by different physical conditions in the atmospheres of the components and the errors in continuum location. The spectral line parameters were taken from the catalog of the VALD system (Ryabchikova et al. 1998; Kupka et al. 1999).

Table 2: *Equivalent widths and iron abundances for component "a" for two dates*

λ,Å	ϵ_i, eV	lg gf	W_λ, mÅ	lg$N(Fe)$	W_λ, mÅ	lg$N(Fe)$
			07.02.2001		06.04.2001	
5262.61	4.32	-2.28	13.6	7.92	17.0	8.06
5263.31	3.27	-0.88	131.0	7.78	128.0	7.74
5266.56	3.00	-0.39	175.6	7.59	166.8	7.51
5267.27	4.37	-1.60	19.5	7.61	10.4	7.22
5269.54	0.86	-1.62	310.1	7.82	233.2	7.41
5270.36	1.61	-1.34	239.4	7.79	206.2	7.54
5273.16	3.29	-0.99	100.8	7.49	90.2	7.33
5273.37	2.48	-2.16	51.3	7.09	100.0	7.84
5277.31	4.42	-1.62	8.9	7.19	5.7	6.91
5281.79	3.04	-0.83	130.2	7.52	140.3	7.64
5283.62	3.24	-0.43	148.5	7.55	201.3	8.06
5285.13	4.44	-1.64	24.5	7.78	14.1	7.56
5288.53	3.70	-1.51	58.1	7.72	50.6	7.60
5320.04	3.64	-2.54	19.9	7.83	16.1	7.73
5321.11	4.34	-0.95	31.9	7.15	24.9	6.97
5322.04	2.28	-2.80	46.4	7.53	53.2	7.62
5324.18	3.21	-0.10	191.8	7.63	188.5	7.60
5326.14	3.57	-2.07	23.7	7.53	28.7	7.62
5327.25	3.64	-2.99	2.8	7.51	8.4	7.79
5328.04	0.92	-1.47	288.9	7.64	342.9	7.86
5328.53	1.56	-1.85	210.9	7.99	169.7	7.49
5329.99	4.08	-1.19	55.3	7.69	52.6	7.64
5331.53	3.64	-3.54	3.7	7.95	7.9	8.51
5331.90	1.56	-2.78	101.1	7.50	100.5	7.49
5339.40	4.34	-1.66	20.7	7.65	20.7	7.65
5339.93	3.27	-0.65	148.2	7.76	134.2	7.60
5341.02	1.61	-1.95	172.5	7.66	166.5	7.58
5349.74	4.39	-1.30	52.9	7.99	52.9	7.99
5353.37	4.10	-0.84	62.5	7.45	93.4	7.96
5379.57	3.70	-1.51	58.8	7.72	56.4	7.69
5383.37	4.31	0.64	157.4	7.54	150.5	7.50
5385.58	3.70	-2.97	5.0	7.64	5.0	7.64
5386.34	4.15	-1.77	22.7	7.65	18.9	7.58
5386.96	3.62	-2.62	17.6	7.81	12.8	7.68
5387.48	4.14	-2.03	19.0	7.74	14.6	7.64
5389.48	4.42	-0.41	91.4	7.76	84.2	7.65
5391.46	4.15	-0.82	82.4	7.80	97.8	8.05
5393.17	3.24	-0.72	121.1	7.47	121.5	7.48
5394.68	4.19	-1.62	28.9	7.69	38.4	7.86
5395.22	4.45	-2.17	13.9	7.93	17.6	8.08
5397.13	4.45	-0.34	106.6	7.94	169.2	8.67
5398.28	4.45	-0.67	67.0	7.67	66.5	7.66
5400.50	4.37	-0.16	68.7	7.11	132.8	8.05
5401.27	4.32	-1.9	18.1	7.74	17.0	7.71
5403.82	4.08	-1.03	83.6	7.98	84.0	7.98
5404.11	4.31	0.22	152.5	7.83	156.2	7.87
5405.35	4.39	-1.39	39.8	7.83	30.0	7.66
5405.77	0.99	-1.84	272.4	7.91	171.7	6.85

Table 2: *Equivalent widths and iron abundances for component "a" for two dates (continued)*

λ,Å	ϵ_i, eV	lg gf	W_λ, mÅ	lg$N(Fe)$	W_λ, mÅ	lg$N(Fe)$
			07.02.2001		06.04.2001	
5406.77	4.37	-1.72	33.1	7.97	30.1	7.91
5407.48	4.08	-1.96	33.3	7.96	38.6	8.08
5441.34	4.31	-1.73	15.8	7.58	24.9	7.76
5445.04	4.39	-0.02	108.2	7.60	112.4	7.65
5446.92	0.99	-1.91	200.7	7.34	194.8	7.26
5448.27	4.14	-1.84	15.1	7.54	24.4	7.72
5452.09	3.64	-2.86	13.9	7.91	6.1	7.60
5455.44	4.32	0.29	113.9	7.34	105.6	7.21
5455.61	1.01	-2.09	182.8	7.29	195.5	7.47
5461.55	4.44	-1.90	18.3	7.82	22.2	7.92
5462.95	4.47	-0.16	99.3	7.67	100.8	7.69
5463.28	4.43	0.11	102.6	7.44	110.7	7.55
5464.28	4.14	-1.40	32.8	7.55	38.1	7.64
5466.39	4.37	-0.63	76.6	7.70	79.5	7.75
5466.99	3.57	-2.23	28.4	7.72	31.2	7.77
5470.09	4.45	-1.81	23.2	7.88	14.4	7.66
5472.71	4.21	-1.50	42.8	7.85	41.7	7.83
5473.16	4.19	-2.14	17.3	7.81	10.8	7.62
5473.90	4.15	-0.76	86.2	7.79	80.6	7.70
5476.29	4.14	-0.92	82.3	7.89	82.0	7.88
5476.56	4.10	-0.45	112.6	7.83	94.2	7.56
5510.22	4.08	-2.77	3.8	7.63	4.4	7.67
5512.26	4.37	-1.42	43.0	7.90	21.3	7.51
5517.06	4.21	-2.37	11.1	7.80	10.5	7.78
5522.45	4.21	-1.55	33.6	7.72	39.6	7.83
5524.25	4.15	-2.83	2.8	7.63	2.8	7.63
5525.12	3.27	-3.95	11.4	6.92	15.0	7.09
5525.54	4.23	-1.08	49.9	7.60	54.4	7.68
5531.98	4.91	-1.61	14.4	7.79	7.7	7.57
5532.75	3.57	-2.15	22.8	7.56	50.7	8.05
5534.85	3.24	-2.73	90.1	7.39	73.1	7.12
5535.42	4.19	-1.16	50.2	7.65	74.8	8.05
5538.52	4.22	-2.07	18.6	7.81	13.4	7.67
5539.28	3.64	-2.66	10.4	7.64	3.1	6.99
5539.83	4.29	-2.53	3.7	7.59	10.2	7.98
5569.62	3.42	-0.49			135.7	7.57
5572.84	3.40	-0.28			170.0	7.71
5573.10	4.19	-1.32			50.6	7.80
5576.09	3.43	-1.00			110.2	7.71
5577.03	5.03	-1.55			7.5	7.59
5579.34	4.23	-2.40			7.5	7.69
5584.76	3.57	-2.32			32.1	7.85
5586.76	3.67	-0.12			165.5	7.74
5587.57	4.14	-1.85			21.5	7.67
5589.00	4.47	-2.85			3.4	7.93
5594.66	4.55	-0.66			45.2	7.33
5595.06	5.06	-1.77			8.7	7.80
5598.30	4.65	-0.37			76.7	7.67

Table 2: *Equivalent widths and iron abundances for component "a" for two dates (continued)*

λ,Å	ϵ_i, eV	lg gf	W_λ, mÅ	lg$N(Fe)$	W_λ, mÅ	lg$N(Fe)$
			07.02.2001		06.04.2001	
5600.22	4.26	-1.42			29.6	7.59
5602.54	4.96	-1.46			11.0	7.62
5602.77	4.15	-1.14			55.0	7.67
5602.94	3.43	-0.85			77.0	7.08

Table 3: *Equivalent widths and iron abundances for component "b" for two dates*

λ,Å	ϵ_i, eV	lg gf	W_λ, mÅ	lg$N(Fe)$	W_λ, mÅ	lg$N(Fe)$
			07.02.2001		06.04.2001	
5262.61	4.32	-2.28	10.6	7.81	10.6	7.81
5263.31	3.27	-0.88	124.8	7.89	102.2	7.55
5266.56	3.00	-0.39	110.2	6.96	201.2	7.90
5267.27	4.37	-1.6	22.8	7.70	13.5	7.49
5269.54	0.86	-1.62	235.1	7.64	204.8	7.43
5270.36	1.61	-1.34	210.4	7.78	231.8	7.90
5273.16	3.29	-0.99	87.8	7.48	90.5	7.48
5273.37	2.48	-2.16	30.3	6.80	66.2	7.49
5277.31	4.42	-1.62	4.9	6.84	9.1	7.22
5281.79	3.04	-0.83	130.2	7.72	145.5	7.86
5283.62	3.24	-0.43	127.5	7.52	149.5	7.69
5285.13	4.44	-1.64	20.5	7.72	17.5	7.64
5288.53	3.70	-1.51	49.1	7.64	42.1	7.50
5320.04	3.64	-2.54	30.9	8.17	19.8	7.85
5321.11	4.34	-0.95	29.9	7.16	29.5	7.13
5322.04	2.28	-2.8	49.4	7.68	45.2	7.59
5324.18	3.21	-0.1	189.8	7.72	219.8	7.88
5326.14	3.57	-2.07	21.7	7.53	23	7.55
5327.25	3.64	-2.99	1.8	7.16	9	7.84
5328.04	0.92	-1.47	205.9	7.35	198.2	7.19
5328.53	1.56	-1.85	200.9	8.21	150.9	7.60
5329.99	4.08	-1.19	77.3	8.17	55.5	7.75
5331.53	3.64	-3.54	8.7	8.54	2.2	7.74
5331.90	1.56	-2.78	75.1	7.43	115.5	8.02
5339.40	4.34	-1.66	12.7	7.49	12.7	7.49
5339.93	3.27	-0.65	126.2	7.68	140.2	7.81
5341.02	1.61	-1.95	142.5	7.68	154.8	7.78
5349.74	4.39	-1.3	50.9	8.03	56.5	8.11
5353.37	4.10	-0.84	72.5	7.73	90.5	8.01
5379.57	3.70	-1.51	56.8	7.78	67.8	7.95
5383.37	4.31	0.64	161.4	7.61	135.4	7.37
5385.58	3.70	-2.97	5	7.64	5	7.64
5386.34	4.15	-1.77	23.7	7.70	20	7.62
5386.96	3.62	-2.62	17	7.83	13.8	7.72
5387.48	4.14	-2.03	16	7.69	10	7.54
5389.48	4.42	-0.41	82.4	7.73	73.8	7.56
5391.46	4.15	-0.82	65.4	7.62	68.8	7.66
5393.17	3.24	-0.72	118.1	7.62	116.8	7.57
5394.68	4.19	-1.62	27.9	7.70	32.8	7.79
5395.22	4.45	-2.17	11.9	7.86	15.9	8.03
5397.13	4.45	-0.34	96.6	7.91	80.2	7.62

Table 3: *Equivalent widths and iron abundances for component "b" for two dates (continued)*

λ,Å	ϵ_i, eV	lg gf	W_λ, mÅ	lg$N(Fe)$	W_λ, mÅ	lg$N(Fe)$
			07.02.2001		06.04.2001	
5398.28	4.45	-0.67	60	7.64	63.2	7.66
5400.50	4.37	-0.16	60.7	7.06	105.2	7.75
5401.27	4.32	-1.9	15.1	7.68	13	7.63
5403.82	4.08	-1.03	52.6	7.55	63	7.71
5404.11	4.31	0.22	125.5	7.65	125.5	7.63
5405.35	4.39	-1.39	34.8	7.79	34.5	7.78
5405.77	0.99	-1.84	190.4	7.58	206.4	7.65
5406.77	4.37	-1.72	35.1	8.07	31.2	7.96
5407.48	4.08	-1.96	25.3	7.83	25.2	7.82
5441.34	4.31	-1.73	32.8	7.97	26	7.82
5445.04	4.39	-0.02	126.2	7.92	128.2	7.95
5446.92	0.99	-1.91	199.5	7.68	162	7.31
5448.27	4.14	-1.84	11.2	7.37	24.8	7.77
5452.09	3.64	-2.86	12	7.86	14.2	7.96
5455.44	4.32	0.29	131.5	7.65	113.8	7.50
5455.61	1.01	-2.09	180.5	7.68	174.8	7.63
5461.55	4.44	-1.9	9.8	7.59	20	7.90
5462.95	4.47	-0.16	100.2	7.78	60	7.13
5463.28	4.43	0.11	91.5	7.39	137	7.94
5464.28	4.14	-1.4	47.8	7.86	51.8	7.94
5466.39	4.37	-0.63	77.8	7.83	85.8	7.96
5466.99	3.57	-2.23	28	7.76	37.8	7.96
5470.09	4.45	-1.81	23.8	7.93	18.2	7.78
5472.71	4.21	-1.5	40.8	7.87	38	7.82
5473.16	4.19	-2.14	18.5	7.87	12	7.67
5473.90	4.15	-0.76	87	7.937	91.5	8.01
5476.29	4.14	-0.92	59.5	7.61	64.8	7.70
5476.56	4.10	-0.45	80.6	7.49	75.8	7.40
5510.22	4.08	-2.77	3.8	7.63	4.4	7.68
5512.26	4.37	-1.42	46.8	8.04	36.5	7.83
5517.06	4.21	-2.37	12.5	7.88	11	7.81
5522.45	4.21	-1.55	33.8	7.78	32.5	7.75
5524.25	4.15	-2.83	4.8	7.81	2.8	7.63
5525.12	3.27	-3.95	17.8	7.35	12.8	7.07
5525.54	4.23	-1.08	69.2	8.02	57.2	7.80
5531.98	4.91	-1.61	6.8	7.55	13.5	7.77
5532.75	3.57	-2.15	39.8	7.93	47.2	8.08
5534.85	3.24	-2.73	97.8	7.73	92	7.63
5535.42	4.19	-1.16	72.2	8.12	80.8	8.27
5538.52	4.22	-2.07	29	8.14	15.2	7.74
5539.28	3.64	-2.66	10.4	7.66	9.1	7.62
5539.83	4.29	-2.53	5	7.68	10.2	8.00
5569.62	3.42	-0.49			130.2	7.67
5572.84	3.40	-0.28			160.2	7.76
5573.10	4.19	-1.32			50.6	7.87
5576.09	3.43	-1			111.2	7.92
5577.03	5.03	-1.55			22.8	8.13
5579.34	4.23	-2.4			14.8	8.03

Table 3: *Equivalent widths and iron abundances for component "b" for two dates (continued)*

λ,Å	ϵ_i, eV	lg gf	W_λ, mÅ	lg$N(Fe)$	W_λ, mÅ	lg$N(Fe)$
			07.02.2001		06.04.2001	
5584.76	3.57	-2.32			34.2	7.96
5586.76	3.67	-0.12			167.5	7.88
5587.57	4.14	-1.85			25.2	7.78
5589.00	4.47	-2.85			3.8	7.99
5594.66	4.55	-0.66			31.2	7.05
5595.06	5.06	-1.77			8.7	7.80
5598.30	4.65	-0.37			56.5	7.41
5600.22	4.26	-1.42			25.2	7.53
5602.54	4.96	-1.46			11	7.62
5602.77	4.15	-1.14			55	7.75
5602.94	3.43	-0.85			77	7.22

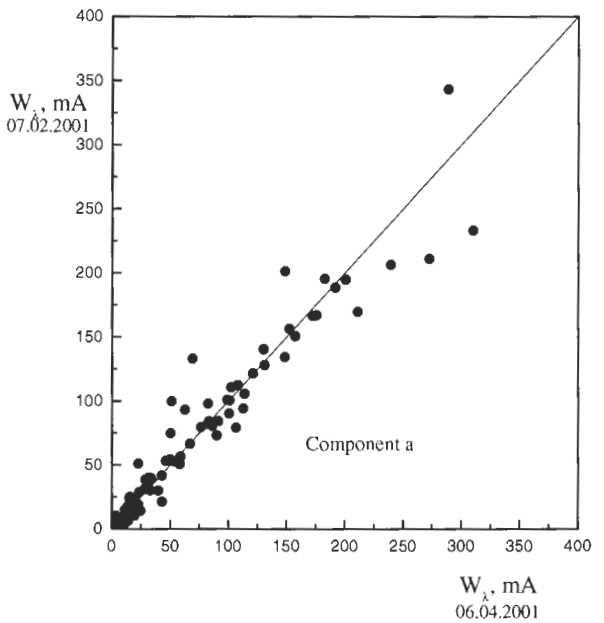

Figure 3: *Comparison of the equivalent widths of the spectra obtained on 07.02.2001 (ordinate) and 06.04.2001 (abscissa) for component "a".*

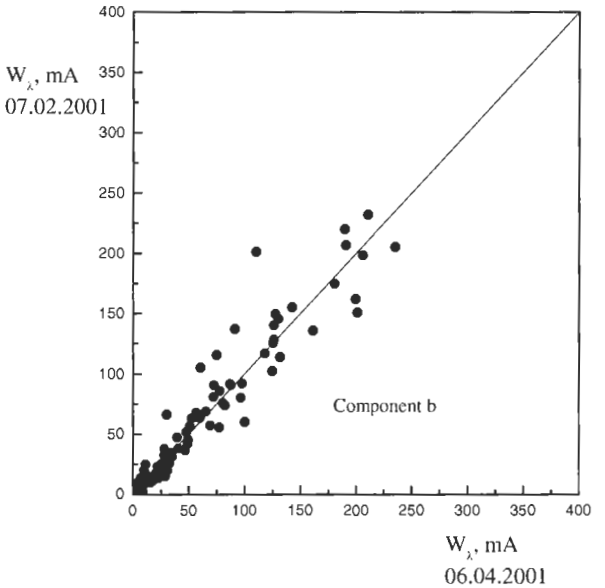

Figure 4: *Comparison of the equivalent widths of the spectra obtained on 07.02.2001 (ordinate) and 06.04.2001 (abscissa) for component "b".*

5. Iron abundance and turbulent velocities in the atmospheres of 41 Dra system

To determine the iron abundances in the atmospheres of the components we have first found equivalent widths of FeI lines in the region $\lambda\lambda 5260 - 5605$ ÅÅ.

The results are presented in Tables 2 and 3, giving the wavelength (λ, Å), the excitation potential of the lower level (ϵ_i, eV), the transition oscillator strengths (lg gf), line equivalent widths measured from our spectra (W_λ, mÅ), and iron abundances (lg $N(Fe)$) found for each line. The model atmospheres were calculated for each component using the parameters of the continuum spectrum (Al-Wardat et al. 2002):

for a $T_{eff} = 6575 \pm 200$ K, lg$g = 4.08 \pm 0.1$,

for b $T_{eff} = 6600 \pm 200$ K, lg$g = 4.26 \pm 0.1$.

The model atmospheres were calculated using the SAM1 program (Wright 1975) and its modified version KONTUR (Leushin & Topilskaya 1985; Leushin 1995) with the solar chemical composition.

Table 4 gives the relative iron abundances for different microturbulence velocities of component a

$$\lg N(Fe) = \lg N(Fe)_0 + k\,[m\text{Å}^{-1}] \cdot W_\lambda[m\text{Å}].$$

Similar data for component b are given in Table 5. These relationships were derived from the spectra obtained before the periastron passage on 07.02.2001

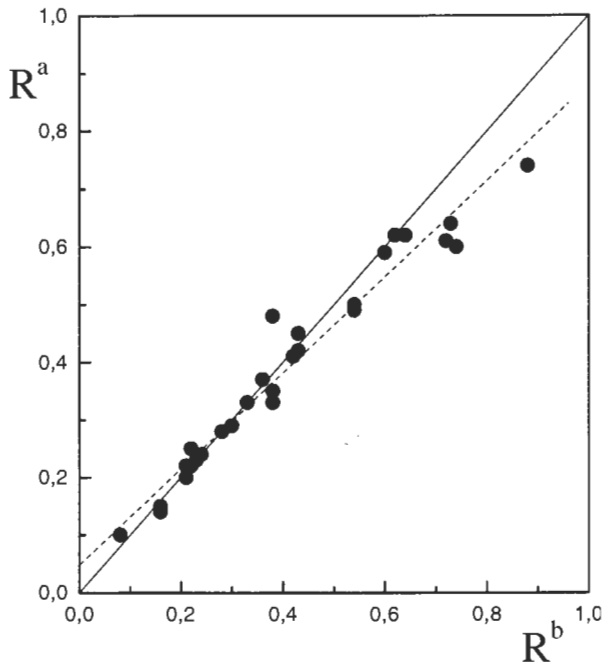

Figure 5: *A comparison of the central line depths in the spectra of components "a" and "b". The middle line (dashes) shows the linear regression* $R^a = 0.833\,R^b + 0.048$.

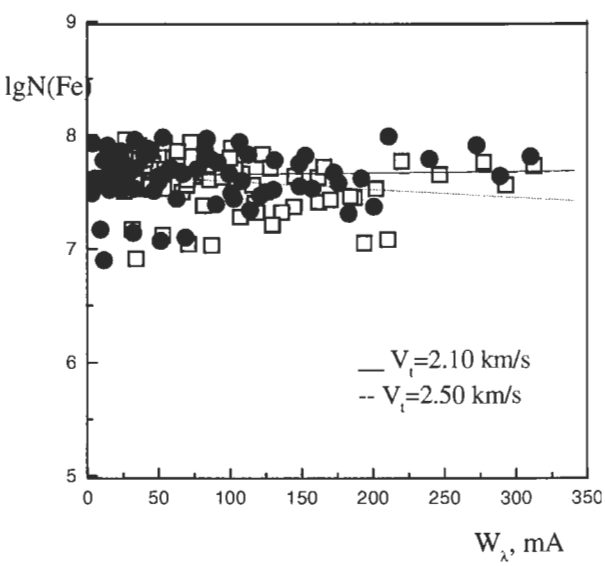

Figure 6: *The value* lg$N(Fe)$ *for different equivalent widths. Dots — Fe abundance obtained for* $V_t = 2.10\,km/s$, *squares — for* $V_t = 2.50\,km/s$.

and 06.04.2001. Two relationships for $V_t = 2.10$ km/s and $V_t = 2.50$ km/s are shown in Fig. 6.

The data, presented in Table 4, show that the microturbulence velocity in the atmosphere of component a is equal to 2.15 ± 0.10 km/s. No variations above the given error were found from our analysis for any phase of the binary.

The most probable microturbulence velocity in the atmosphere of component "b" is $V_t = 1.70 \pm 0.10$ km/s. Therefore, the difference of microturbulence velocities of the components confirms the difference in their gravities obtained from the continuum spectra. At the same time, under similar equivalent widths, the smaller value of the microturbulence velocity leads to deeper spectral lines. This conclusion is illustrated in Fig. 5. The abundances, given in Tables 2 and 3, were obtained with the microturbulence velocity $V_t = 2.15$ km/s for component a, and $V_t = 1.70$ km/s for component b.

For both components the mean values of lgN(Fe) agree within their internal errors:

$$\text{for } a \quad \lg N(Fe) = 7.666 \pm 0.033,$$

$$\text{for } b \quad \lg N(Fe) = 7.706 \pm 0.033.$$

6. FeII lines

A part of iron in the atmospheres of 41 Dra components is in the ionized state. However, FeII lines are not numerous in the spectrum. The averaged values of FeII line equivalent widths for components a and b are given in Table 6 for all the spectra from Table 1. These values are compared in Fig. 7, which shows a coincidence of equivalent widths within their error bars. At the same time, the following possible relationship

$$W_\lambda{}^b = 1.042 \cdot W_\lambda{}^a - 0.634$$

indicates a small rise of line intensities in the spectrum of component b for larger equivalent width, which confirms a slightly higher effective temperature for b in comparison with a. Table 7 summarizes the results of microturbulence velocity measurements and iron abundances found from FeII lines in the spectra of both components.

The iron abundance from the FeII lines agrees with the abundance found for FeI:

$$\text{for } a \quad \lg N(Fe) = 7.638 \pm 0.037,$$

$$\text{for } b \quad \lg N(Fe) = 7.746 \pm 0.027.$$

Note that the difference in lg $N(Fe)$ for components a and b from FeII lines is higher than the formal internal errors. Microturbulence velocities from FeI and FeII lines are essentially the same. The components of 41 Dra have relatively thin atmospheres in which the effective depths of line formation for different ions differ very slightly. Fig. 8 shows the dependence of the effective depths of FeI and FeII line formation on their equivalent widths. Computations were made for component a with our model atmosphere at the wavelength $\lambda 5500$ Å. The comparison of the optical and geometrical depths is also given in

Table 4: *Relative iron abundance for different microturbulence velocities and corresponding mean values of* $\lg N(Fe)$ *for component "a" for two different dates*

	FeI $\lambda\lambda 5260 - 5605$							
V_t, km/s	07.02.2001				06.04.2001			
	k	$\lg N(Fe)_0$	$\lg N(Fe)$	$\pm\Delta(\lg N)$	k	$\lg N(Fe)_0$	$\lg N(Fe)$	$\pm\Delta(\lg N)$
1.50	+0.00087	7.660	7.723	0.037	+0.00116	7.717	7.799	0.034
2.00	+0.00060	7.664	7.680	0.035	+0.00052	7.702	7.720	0.034
2.10	+0.00011	7.666	7.674	0.032	+0.00011	7.682	7.672	0.033
2.15	+0.00001	7.664	7.665	0.035	-0.00011	7.675	7.667	0.035
2.20	-0.00008	7.661	7.655	0.037	-0.00090	7.670	7.663	0.036
2.50	-0.00067	7.650	7.601	0.043	-0.00095	7.668	7.601	0.037

Table 5: *Relative iron abundance for different microturbulence velocities and corresponding mean values of* $\lg N(Fe)$ *for component "b" for two different dates*

	FeI $\lambda\lambda 5260 - 5605$							
V_t, km/s	07.02.2001				06.04.2001			
	k	$\lg N(Fe)_0$	$\lg N(Fe)$	$\pm\Delta(\lg N)$	k	$\lg N(Fe)_0$	$\lg N(Fe)$	$\pm\Delta(\lg N)$
1.50	+0.00034	7.717	7.739	0.047	+0.00041	7.735	7.762	0.037
1.60	+0.00017	7.710	7.720	0.046	+0.00023	7.728	7.723	0.037
1.70	-0.00001	7.701	7.700	0.045	-0.00012	7.720	7.712	0.033
1.80	-0.00021	7.695	7.682	0.046	-0.00018	7.714	7.702	0.035
1.90	-0.00040	7.688	7.662	0.046	-0.00040	7.710	7.683	0.036

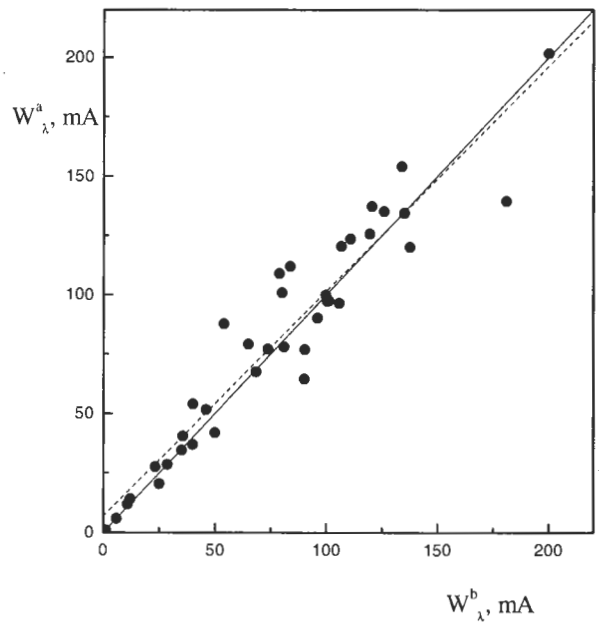

Figure 7: *A comparison of the equivalent widths of FeII lines in the spectra of components a and b. The middle line (dashes) shows the linear regression* $W^b_\lambda = 1.042 \times W^a_\lambda - 0.634$.

Fig. 8. The effective depth of line formation (τ_w) is defined by the relationship:

$$\tau_w = \int_0^\infty (1 - r_\lambda)\tau_\lambda d\lambda \Big/ \int_0^\infty (1 - r_\lambda) d\lambda,$$

where

$$\tau_\lambda = \int_0^\infty S_\lambda(t) E_2(t) t\, dt \Big/ \int_0^\infty S_\lambda(t) E_2(t)\, dt$$

gives the depth of a flux formation in the line.

It can be seen from Fig. 8 that FeI lines form in the atmosphere higher than FeII lines, however, the difference is not significant. In the linear scale, the difference of the altitudes is of the order of 10 km for a line with $W_\lambda = 70\,m$Å ($\Delta\tau = 0.05$), while all the atmosphere is extended to about 200 km.

Table 6: *Equivalent widths of FeII line and iron abundances for components "a" and "b" and the Sun*

λ,Å	ϵ_i, eV	lg gf	W_λ, mÅ	lg$N(Fe)$ component a	W_λ, mÅ	lg$N(Fe)$ component b	W_λ, mÅ ($\odot$ $T_{eff} = 5770, \lg g = 4.41$)	lg$N(Fe)$
4124.79	2.54	-4.20	54.1	7.82	40.1	7.68	33	7.66
4128.74	2.58	-3.77	79.3	7.88	65.0	7.80	50	7.68
4303.17	2.70	-2.67	123.5	7.65	110.8	7.67	103	7.66
4385.38	2.78	-2.61	137.1	7.84	120.4	7.80	81	7.38
4489.18	2.89	-3.15	108.9	8.00	78.8	7.64	61	7.58
4508.28	2.86	-2.31	120.0	7.35	137.5	7.77	84	7.15
4515.34	2.84	-2.48	134.4	7.70	135.0	7.89	75	7.14
4520.23	2.79	-2.74	96.4	7.27	105.8	7.67	69	7.25
4522.63	2.84	-2.22	125.6	7.34	119.5	7.50	101	7.34
4541.52	2.84	-2.93	112.0	7.77	83.8	7.48	58	7.25
4549.47	2.83	-2.05	135.1	7.31	126.0	7.41	231	8.02
4555.89	2.82	-2.42	154.0	7.87	133.8	7.79	77	7.09
4576.33	2.83	-3.04	97.4	7.59	101.2	7.91	66	7.53
4582.84	2.83	-3.26	100.8	7.88	80.0	7.71	49	7.35
4583.83	2.79	-1.87	201.6	7.75	200.0	7.81	124	7.14
4620.52	2.83	-3.29	64.5	7.24	90.2	7.94	56	7.54
4635.32	5.95	-1.58	34.6	7.64	35.0	7.73	14	7.51
4656.98	2.89	-3.66	67.5	7.74	68.5	7.94	34	7.41
4666.75	2.82	-3.33	90.2	7.73	96.0	8.09	45	7.29
4670.18	2.58	-4.11	40.5	7.42	35.5	7.45	27	7.36
4993.35	2.81	-3.70	87.7	8.02	54.0	7.58	34	7.35
5000.74	2.78	-4.61	28.6	7.78	28.6	7.87	12	7.56
5100.66	2.81	-4.22	37.0	7.65	40.0	7.80	17	7.36
5234.63	3.22	-2.27	120.4	7.49	106.8	7.50	87	7.48
5264.79	3.25	-3.23	77.1	7.72	73.8	7.84	47.2	7.62
5272.40	5.96	-2.03	20.5	7.69	25.0	7.86	9.5	7.66
5284.11	2.89	-2.99	99.8	7.53	99.8	7.75	67	7.5
5316.62	3.15	-1.85	139.5	7.30	181.0	7.83	112	7.29
5316.78	3.22	-2.76	97.2	7.55	100.5	7.82	97	8.02
5325.55	3.22	-3.32	78.0	7.80	81.0	8.04	45	7.64
5337.73	3.23	-3.89	51.6	7.91	46.0	7.93	35	7.94
5414.08	3.22	-3.48	42.0	7.29	50.0	7.61	27.5	7.31
5508.26	6.70	-3.10	1.0	7.79	1.2	7.88	0.5	7.86
5525.13	3.27	-3.94	27.6	7.56	23.2	7.55	13	7.33
5529.93	6.73	-1.88	11.9	7.78	10.8	7.78	5	7.77
5534.85	3.24	-2.73	76.8	7.18	90.2	7.60	63	7.47
5567.84	6.73	-1.89	14.1	7.88	12.0	7.84	4	7.69
5591.37	3.27	-4.68	5.9	7.52	5.9	7.55	7	7.67

Table 7: *Relative iron abundance for different turbulence velocities and corresponding mean values of lg $N(Fe)$ with their internal errors*

V_t, km/s	k	lg$N(Fe)_0$	lg$N(Fe)$	$\pm\Delta$(lg$N$)	V_t, km/s	k	lg$N(Fe)_0$	lg$N(Fe)$	$\pm\Delta$(lg$N$)
Component a					Component b				
1.70	+0.00096	7.704	7.782	0.038	1.50	+0.00052	7.761	7.803	0.028
2.15	-0.00037	7.668	7.638	0.037	1.70	+0.00013	7.735	7.746	0.027
2.50	-0.00152	7.663	7.539	0.040	2.00	-0.00059	7.704	7.658	0.029

Table 8: *Equivalent widths and iron abundances for component "a" of 41 Dra and the Sun*

λ, Å	ϵ_i, eV	lg gf	W_λ, mÅ	lg$N(Fe)$	W_λ*, mÅ	lg$N(Fe)_\odot$ **	lg$N(Fe)_\odot$*
5225.53	0.11	-4.79	71.1	7.55	70.3	7.24	7.478
5326.14	3.57	-2.07	25.9	7.57	34.5	7.29	7.426
5412.79	4.44	-1.72	23.5	7.81	19.1	7.34	7.486
5600.23	4.26	-1.42	29.6	7.59	36.5	7.33	7.444
6200.32	2.61	-2.44	59.1	7.58	75.4	7.58	7.559
6219.29	2.2	-2.43	90.2	7.56	91	7.48	7.474
6232.65	3.65	-1.22	85	7.71	88.4	7.58	7.432
6240.65	2.22	-3.23	36.3	7.63	47.6	7.37	7.442
6265.14	2.18	-2.55	92.4	7.67	86.7	7.5	7.479
6271.29	3.33	-2.7	17.6	7.65	20.5	7.21	7.406
6593.88	2.43	-2.42	83.2	7.74	86.5	7.55	7.532
6609.12	2.56	-2.69	51.2	7.63	65.3	7.54	7.526
6945.41	2.42	-2.48	81	7.64	83.2	7.52	7.492
6978.86	2.48	-2.5	86.8	7.78	79.9	7.53	7.501
7401.69	4.19	-1.6	36	7.71	41.9	7.51	7.548

* — values from Grevesse and Sauval (1999),
** — values calculated by us for the Sun (T_{eff} = 5770, lg g=4.44, V_t = 0.85 km/s).

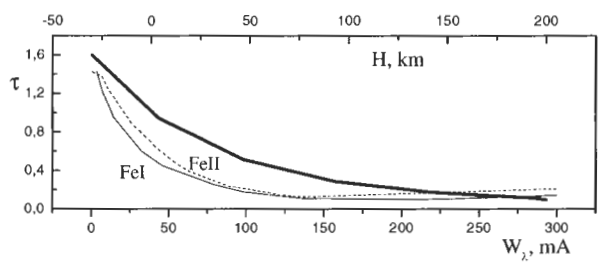

Figure 8: *Effective depth of the spectral line formation as a function of its equivalent width for FeI (solid thin line) and FeII (dashes). The thick solid line shows the relation of the geometrical depth (H) and the optical depth (τ) for the model with T_{eff} = 6575 K and* lg g=*4.08.*

7. Comparison of the iron abundance in the atmospheres of the Sun and 41 Dra

The weighted mean values for the iron abundances in the atmospheres of 41 Dra components are:

$$\text{for } a \ \lg N(Fe) = 7.66 \pm 0.03,$$

$$\text{for } b \ \lg N(Fe) = 7.72 \pm 0.03.$$

The weights are chosen with account for the number of ion lines used, correspondingly 3:1 for FeI and FeII. Comparison of our abundances with the solar composition, lg $N(Fe)_\odot = 7.50 \pm 0.05$ (Grevesse and Sauval 1999), shows a small iron excess for 41 Dra. This difference is 0.16 dex and 0.22 dex for components a and b, correspondingly. This difference fits well the spread of values for individual lines. Table 8 gives the comparison between our lg $N(Fe)$ measurements for 41 Dra and solar abundances for coinciding lines. Here, columns 4 and 5 give the equivalent widths for FeI lines and corresponding lg $N(Fe)$ for component a, column 6 presents equivalent widths for the Sun (Grevesse and Sauval 1999), column 7 shows our lg $N(Fe)_\odot$ calculations for the Sun with T_{eff} = 5770, lg g = 4.44, V_t = 0.85 km/s, the last column gives the corresponding values from Grevesse and Sauval (1999). The mean difference for these lines is

$$\lg N(Fe)_{41\,Dra} - \lg N(Fe)_\odot = 7.66 - 7.48 = 0.18.$$

In addition to the 41 Dra data, Table 6 includes solar equivalent FeII widths (Moore et al. 1966) together with our calculations of lg $N(Fe)_\odot$ for the same solar model atmosphere. The mean solar iron abundance value found from FeII lines is

$$\lg N(Fe)_\odot = 7.50 \pm 0.05,$$

which perfectly agrees with the results of Grevesse and Sauval (1999). Therefore we may conclude that the iron abundance is 0.16 dex higher in the atmosphere of 41 Dra a than in the solar atmosphere, while for 41 Dra b the difference is +0.22 dex.

8. Conclusions

The analysis of FeI and FeII spectral lines in the atmospheres of 41 Dra a and b components confirms the

speckle interferometric intensity ratio $E^b/E^a = 0.68$ and, possibly, testifies a higher effective temperature of the secondary star. Iron abundances in the atmospheres of both components are practically identical and slightly higher than the solar abundance. No significant difference in the iron abundances for FeI and FeII lines was found. However, it should be noted that the low overabundance of Fe that we have found may be related to the overestimation of the temperature values of the components. The effective temperatures determined from B-V and energy distribution may be by 100-200 K lower than those we use (Balega et al. 2001).

A difference of the components microturbulence velocities of $V_t{}^a - V_t{}^b = 0.45\,\mathrm{km/s}$ confirms different gravities at their surfaces: $\lg g = 4.08$ for a, and $\lg g = 4.26$ for b.

Acknowledgements. The study was made with a financial support obtained from the RFBR (grants no.00-02-16213 and no.01-02-16563).

References

Balega Yu.Yu., 1997, Pis'ma Astron. Zh., **23**, 199
Balega Yu.Yu., Leushin V.V., Pluzhnik E.A., 2001, Bull. Spec. Astrophys. Obs., **51**, 61
Grevesse N. and Sauval A.J., 1999, Astron. Astrophys., **347**, 348
Galazutdinov G.A., 1992, SAO Preprint, **92**
Kupka F., Piskunov N.E., Ryabchikova T.A., Stempels H.C., Weiss W.W., 1999, Astrophys. J. Suppl. Ser., **138**, 119
Leushin V.V., 1995, Astron. Zh., **72**, 543
Leushin V.V., Topilskaya G.P., 1985, Astrofizika, **22**, 121
Moore C.E., Minnaert M.G.J., Houtgast J., 1966, The Solar Spectrum 2935 Å to 8770 Å. NBS Monograph 61. Washington
Musaev F.A., 1993, Pis'ma Astron. Zh., **19**, 776
Panchuk V.E., Najdenov I.D., Klochkova V.G., Ivanchik A.B., Ermakov S.V., Murzin V.A., 1998, Bull. Spec. Astrophys. Obs., **44**, 127
Ryabchikova T.A., Piskunov N.E., Stempels H.C., Kupka F., Weiss W.W., 1998, Physica Scripta. Proc. of ASOS6, **T83**, 162
Wright S.L., 1975, Comm. Univ. London Obs., **76**, 1